Romanian Reports in Physics **70**, 402 (2018)

BROADLY PEAK POWER AND PULSE WIDTH TUNABLE DISSIPATIVE SOLITON RESONANCE GENERATION IN FIGURE OF EIGHT FIBER LASER

M. SALHI[1,*], G. SEMAAN[1], F. BEN BRAHAM[1,2,3], A. NIANG[1], F. BAHLOUL[2], F. SANCHEZ[1]

[1] Université d'Angers, Laboratoire de Photonique d'Angers E. A. 4464, 2 Bd Lavoisier, 49045 Angers Cedex 01, France
[2] Université de Carthage, Laboratoire Systèmes Électroniques et Réseaux de Communications (SERCOM), École Polytechnique de Tunisie, EPT, B.P. 743, 2078, Tunisie
[3] Université de Tunis El Manar, École Nationale d'Ingénieurs de Tunis, 1002, Tunisie
[*]*Corresponding author*: mohamed.salhi@univ-angers.fr

Received September 15, 2017

Abstract. We experimentally demonstrate a broadly tunable dissipative soliton resonance dual-amplifier figure-of-eight fiber laser emission. The peak power is tuned continuously from 8.8 to 41.4 W by the first amplifier and pulse width from 84 to 416 ns by the second one.

Key words: dissipative soliton resonance, figure-of-eight fiber laser, tunable laser.

1. INTRODUCTION

The demand grows more and more on energetic pulsed fiber lasers for a wide variety of industrial and scientific applications including material processing, medical equipment, nonlinear microscopy and more [1, 2]. The strong interest in this kind of lasers is due to their several inherent advantages offered in terms of stability, compactness, high-energy and ease-of-use. However, achieving microjoule energies directly from laser oscillator with dissipative solitons is not possible because of several physical mechanisms. Indeed, depending on the dispersion regime, two energy-limiting phenomena occur. Therefore, the single pulse can be breakup or evolves toward a multiple pulse operation [3]. In the anomalous dispersion regime, the peak power is clamped due to the saturation of the mode-locking mechanism. In that case, the duration and energy are determined by the soliton area theorem. Thus, the pulse energy is quantized. In the normal dispersion regime, the pulse energy is limited by the nonlinear losses combined with the finite gain bandwidth.

Because of physical limitations of single pulse energy, finding techniques capable of overcoming these problems become a real challenge. Several ways have

been explored to develop energetic pulses such as the usage of large mode-area photonic crystal fibers, chirped pulse amplification and beam shaping [4–6]. Square pulse belongs to beam shaping and can be realized by exploiting the dissipative soliton resonance (DSR). Indeed, under the DSR regime, the energy is not limited and it increases proportionally with pumping power; the pulse width widens linearly while the peak power remains constant as it has been theoretically predicted [7, 8]. The first DSR experiment in a net normal dispersion fiber ring laser was reported in 2009 where 281.2 nJ of pulse energy was obtained [9]. Well before that date, in 1991, nanosecond square pulses were observed in a figure-of-eight fiber laser (F8L) [10]. Thereafter, based on the nonlinear amplifying loop mirror (NALM), numerous works have been done on DSR square-wave pulses [11, 12]. Wang and co-workers [11] reported the generation of DSR square-wave pulses with pulse energy of 3.25 nJ and a duration of 73.73 ns in negative group-velocity dispersion. The square-wave pulse DSR generation has also been reported in a positive group-velocity dispersion with high energy of 379.2 nJ and a duration of 363.9 ns [12].

In order to control separately the pulse width and amplitude of DSR, an original laser architecture of dual pump passively mode-locked fiber laser was proposed by Mei *et al*. in Ref. [13]. Indeed, the pulse duration and amplitude may be tuned continuously with two separate fiber amplifiers. Based on a similar configuration and using a dual-amplifier double-clad figure-of-eight Er:Yb co-doped fiber laser, we present a widely tunable pulse energy square-wave pulse. The peak power can be tuned from 8.8 to 41.4 W and the pulse duration from 84 ns to 416 ns. Under optimized conditions, a high energy of 10.1 μJ is obtained.

2. EXPERIMENTAL SETUP

The experimental arrangement is schematically represented in Fig. 1. It consists of a unidirectional amplifying loop (UAL) connected to a NALM by a fiber coupler with a coupling ratio *k*. The DSR is achieved thanks to the action of NALM, which acts as a fast-effective saturable absorber. The UAL is composed of a C-band double-clad co-doped Er:Yb 30 dBm fiber amplifier (A1) from Keopsys (KPSOEM-C-30-BO-RARE). It is pumped with the v-groove technique by laser diodes emitting about 3.5 W of maximum output power at 980 nm. This amplifier has a double clad fiber (DCF) of 2.45 m and a second-order dispersion β_2 = = –0.021 ps^2/m. A polarization insensitive isolator (PI-ISO) is inserted between the amplifier and the 99% output coupler (OC) to ensure the unidirectionality of the loop. The NALM is composed of a second C-band double-clad co-doped Er:Yb 30 dBm fiber amplifier (A2) from Keopsys (KPS-BT2-C-30-BOFA) containing 8 m of DCF with a

maximum available pumping power of about 5 W at 980 nm. Additional coils of SMF28 fiber (L1 ~ 1000 m and L2 ~ 500 m with a second-order dispersion $\beta_2 = -0.022$ ps^2/m) are inserted in the UAL and NALM to increase the nonlinearities. Polarization controllers (PC) in both loops are used to facilitate mode-locking in the cavity. The pulse characteristics are measured using a high-speed photodetector (TIA-1200), a fast oscilloscope (Tektronix TDS 6124C, 12 GHz, 40 GS/s), an integrating sphere (Thorlabs S146C) connected to a digital monitor (Thorlabs PM-100D), an optical spectrum analyzer (Anritsu MS 9710C) and an electronic RF spectrum analyzer (Rohde & Schwarz FSP Spectrum Analyzer 9 kHz to 13.6 GHz).

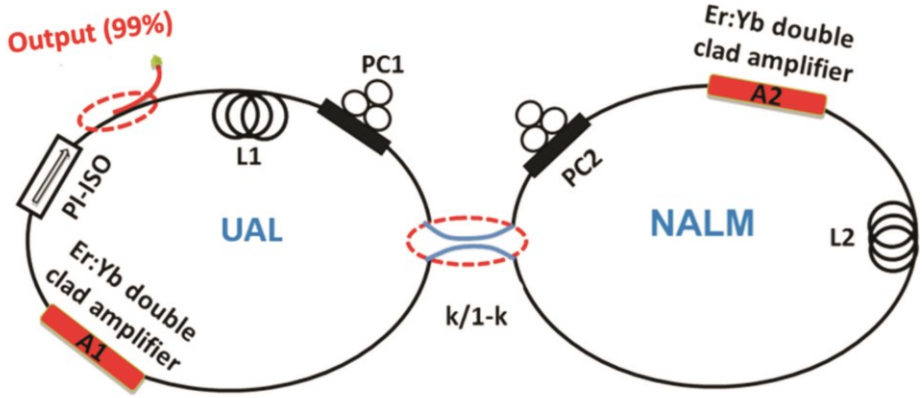

Fig. 1 – Experimental setup of the dual-amplifier figure-of-eight fiber laser.

3. EXPERIMENTAL RESULTS

Using optical configuration employed by our group in [14], we begin by exploring the influence of the central coupling ratio *k* on the DSR characteristics and in particular on the tuning of the peak power and pulse width. The total cavity length is about 1536 m, including 1500 m of SMF28 (L1 ~ 1000 m and L2 ~ 500 m). The net cavity dispersion is −33.23 ps^2, and the round-trip time is 7.65 μs corresponding to a free spectral range of 131 kHz. The passively mode-locked generation of DSR square pulses is obtained at a pump power of A1 = 500 mW in the UAL and A2 = 700 mW in the NALM. Below this pumping threshold, the resonator tends to be unstable and mostly emits noise-like pulses. As we have pointed out in [14], the peak power of the pulse increases linearly with the pump power of A1 without pulse width variation for a fixed pump power of A2, while the pulse width increases linearly with the pump power of A2 at a constant peak power if A1 is turned off, or a variable peak power if A1 is turned on. It is worth to recall that the cavity

operates in the DSR regime as it is presented in Fig. 2 [14]. Figure 2a gives the evolution of the pulses as a function of the pumping power of A1 for a fixed pump power of A2 = 1.7 W while Fig. 2b shows the evolution of the pulses *versus* A2 for pump power of A1 = 3 W. The energy depends linearly on the pumping power of both amplifiers while the pulse width depends linearly and strictly on A2. We have also verified that the spectral bandwidth remains above a significant value as it must be in DSR regime [14]. In addition, the low frequency spectrum exhibits a signal to noise ratio around 60 dB thus demonstrating the very good stability of the mode-locked regime.

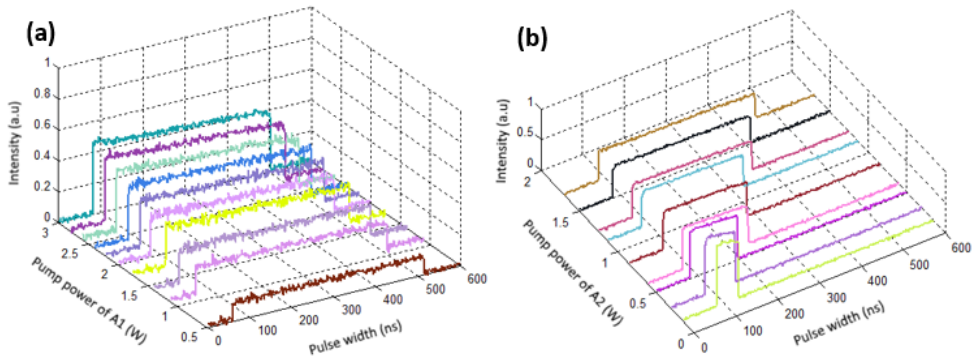

Fig. 2 – Oscilloscope trace of square-wave pulse: a) temporal trace evolution *versus* pumping power of A1; b) temporal trace evolution *versus* pumping power of A2.

To study the influence of the coupling ratio (k) of the central coupler, we first fix the pump power of A2 at 1.8 W, and tune the pumping of A1 from 0.5 W to 3.5 W for different values of k. The evolution of both peak power and pulse energy is presented in Fig. 3. Regardless the value of k, both peak power and pulse energy increase linearly *versus* the pumping power of A1 confirming the DSR regime of the cavity. The best peak power tuning performance has been obtained for k = 0.6. Indeed, in that case, the pulse amplitude can be tuned in a range of 32.6 W, from 8.8 W to 41.4 W while the pulse energy varies from 2.2 µJ to 10.1 µJ. The last value constitutes a record for square-wave pulses in all-fiber laser configuration. It is worth to mention that for a fixed value of k and a given pumping power of A2, the pulse width remains constant for any pump power of A1.

In the second part of the experiment, we fix the pump power of A1 at 3.5 W and we tune pump power of A2 from 0.2 W till 1.8 W. We are limited to the last value for A2 because above 1.8 W the DSR instabilities occur. The evolution of the pulse characteristics is summarized in Fig. 4. Regardless the coupling ratio of the central coupler, as we increase the pumping power of A2, pulse width increases

linearly while peak power decreases in such a way that the energy of the square pulses increases linearly as it has been described in [14].

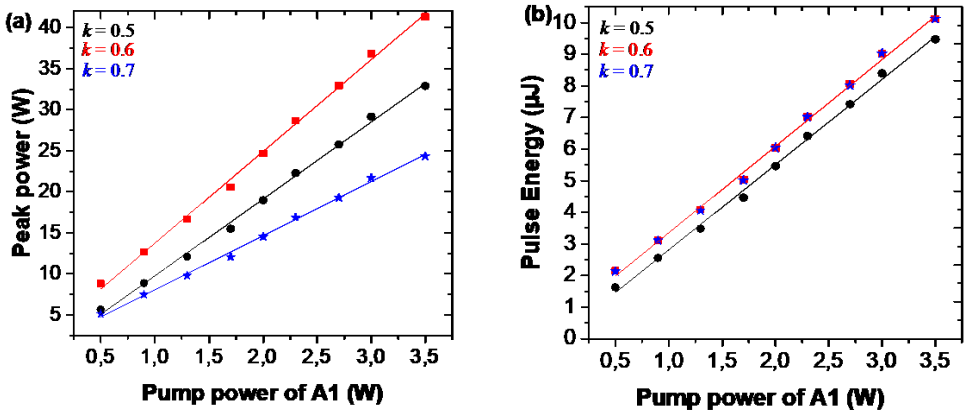

Fig. 3 – a) Peak power and b) pulse energy *versus* pump power of A1 for the different central coupling ratios k at A2 = 1.8 W. The straight lines are linear fits.

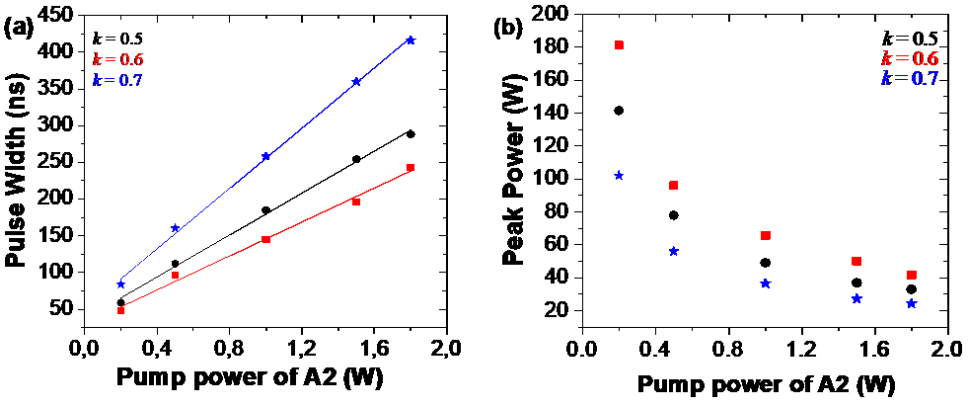

Fig. 4 – a) Pulse width and b) peak power *versus* pump power of A2 for different central coupling ratios k at A1 = 3.5 W. The straight lines are linear fits.

Based on the results presented in Fig. 4, we can deduce that the best performances in term of pulse duration tunability is obtained for the coupling ratio k = 0.7. In such case, the pulse duration can be continuously tuned in a range of 332 ns (84 ns–416 ns). The maximum achievable energy is 10.1 μJ with a pulse width of 416 ns and a peak power of 24.3 W. For k = 0.8 and k = 0.9, multi-pulsing instabilities occur and it is very hard to obtain a stable square-wave pulse. On the other hand, we did not use lower coupling coefficients between the two loops in

order to avoid damages of the amplifier A2 by sending it a higher power on the output port.

4. CONCLUSION

In conclusion, by using dual-amplifier figure-of-eight fiber laser, we have demonstrated in terms of peak power and pulse width, a widely tunable DSR mode-locked Er:Yb doped double-clad fiber laser. Depending on the amplifiers and the central coupling ratio *k,* the tuning range of the peak power is from 8.8 to 41.4 W, and variation of the pulse duration is from 84 to 416 ns. At a total pump power of 5.3 W, the best energy performance of 10.1 μJ with 131 kHz repetition rate is obtained, which is currently the record for square-wave pulses in all-fiber laser configuration.

REFERENCES

1. B. N. Chichkov, C. Momma, S. Nolte, F. von Alvensleben, and A. Tünnermann, Appl. Phys. A **63**, 109–115 (1996).
2. H. Jelinkova, J. Pasta, M. Nemec, J. Sulc, M. Miyagi, Y. W Shi, Y. Matsuura, and M. Jelinek, Laser Phys. **13**, 735–742 (2003).
3. K. Guesmi, G. Semaan, M. Salhi, Y. Meng, F. Bahloul, H. Leblond, and F. Sanchez, Rom. J. Phys. **61**, 1330–1338 (2016).
4. M. Baumgartl, F. Jansen, F. Stutzki, C. Jauregui, B. Ortaç, J. Limpert, and A. Tünnermann, Opt. Lett. **36**, 244-246 (2011).
5. Y. Wang, L. Li, and L. Zhao, Laser Phys. **27**, 035102 (2017).
6. B. Ortaç, A. Hideur, C. Chedot, M. Brunel, G. Martel, and J. Limpert, Appl. Phys. B **85**, 63–67 (2006).
7. W. Chang, A. Ankiewicz, J. M. Soto-Crespo, and N. Akhmediev, Phys. Rev. A **78**, 023830 (2008).
8. W. Chang, A. Ankiewicz, J. M. Soto-Crespo, and N. Akhmediev, J. Opt. Soc. Am. B **25**, 1972–1977 (2008).
9. X. Wu, D. Y. Tang, H. Zhang, and L. M. Zhao, Opt. Express **17**, 5580–5584 (2009).
10. D. J. Richardson, R. I. Laming, D. N. Payne, V. Matsas, and M. W. Phillips, Electron. Lett. **27**, 542–544 (1991).
11. S. K. Wang, Q. Y. Ning, A. P. Luo, Z. B. Lin, Z. C. Luo, and W. C. Xu, Opt. Express **21**, 2402–2407 (2013).
12. J. Yang, C. Guo, S. Ruan, D. Ouyang, H. Lin, Y. M. Wu, and R. Wen, IEEE Photonics J. **5**, 1500806 (2013).
13. L. Mei, G. Chen, L. Xu, X. Zhang, C. Gu, B. Sun, and A. Wang, Opt. Lett. **39**, 3235–3237 (2014).
14. G. Semaan, F. B. Braham, J. Fourmont, M. Salhi, F. Bahloul, and F. Sanchez, Opt. Lett. **41**, 4767–4770 (2016).